

pubs.acs.org/Macromolecules Article

Fully Biobased High-Molecular-Weight Polyester with Impressive Elasticity, Thermo-Mechanical Properties, and Enzymatic Biodegradability: Replacing Terephthalate

Pranabesh Sahu,* Lav Sharma, Tim Dawsey, and Ram K. Gupta*



Cite This: Macromolecules 2024, 57, 9302-9314

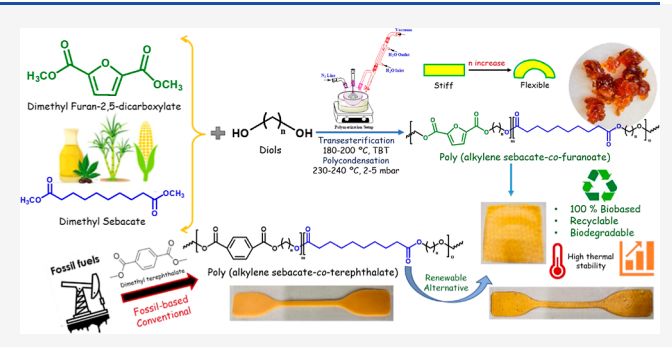


ACCESS I

Metrics & More

Article Recommendations

ABSTRACT: The widespread utilization of petroleum-based plastics causes severe environmental and health issues, prompting the production of biobased high-performance polymers for a sustainable future. This work attempts to develop 100% eco-friendly polymers with comparable properties and the advantages of petro-based plastic, which may find useful applications in beverage packaging. A series of poly(alkylene sebacate-co-furanoate) copolyesters were synthesized using a two-stage melt polycondensation reaction utilizing biomass-derived substituents. Dimethyl furan 2,5-carboxylate and dimethyl sebacate, and different diols such as a 1,4-butane diol or 1,5-pentane diol were used for the synthesis of fully biobased polyester, namely



poly(butylene sebacate-co-furanoate) (PBSF) and poly(pentylene sebacate-co-furanoate) (PPeSF). Solution viscosity, gelpermeation chromatography, FT-IR, and NMR spectroscopies confirm the formation of typical high-molecular-weight aliphaticaromatic polyesters. The glycol chain length played a key role in forming high molecular weight polymers and affected the crystalline, rheological, and thermomechanical properties. Thermal investigations revealed a decrease in the melting and glass-to-rubber transition temperatures as well as a reduction in the crystallization capability with different glycol-chain lengths, a possible odd—even effect phenomenon. Compared to terephthalate-based copolyesters, furan-derived polyesters' higher molecular weight, asymmetric, and nonplanar ring structure suffered significant chain entanglements, strengthening their elasticity, as validated by the rheological properties. Furthermore, biobased copolyester was successfully processed into films and characterized for mechanical, elastic recovery, and enzymatic degradation properties. From mechanical performance and enzymatic degradation studies, furan-derived polyester exhibited impressive elasticity upon stretching and good degradation capabilities compared to its terephthalate counterpart. PBSF exhibited remarkable extensibility with elongation of more than 600% and tensile strength of 8.4 MPa with an excellent recovery rate of 70% (to the original state) after stretching. These aliphatic-aromatic polyesters are biobased and can offer both mechanical and biodegradable alternatives to petroleum-based terephthalate counterparts or commercial polyester poly(butylene adipate-co-terephthalate).

1. INTRODUCTION

The polymer industry's dependence on petroleum-based precursors results in a huge production of synthetic polymers, which contributes to the pervasive plastic pollution in landfills and oceans. This has further worsened with time and calls for the urgent exploration of environmentally benign alternatives. Indeed, it is predicted that worldwide plastics production will reach 34 billion metric tons by 2050, leading to a corresponding 70% rise in global plastic waste above present levels. The majority of synthetic plastics currently on the market are made from petroleum resources, which use many fossil fuels. Plastic waste from food packaging, characterized by a short life cycle and a difficult and expensive recycling process, undermines the ability to meet the carbon emission limits required to combat climate change for the United Nations

Sustainable Development Goals.³ Reusing plastic garbage is the most effective way to manage it, which is necessary for the long-term objectives of moving toward a sustainable economy and circularity in plastics. The nonbiodegradable nature of plastics results in so-called "white pollution", which in turn drives researchers to develop biobased alternatives or biodegradable plastics.^{4,5}

Received: May 10, 2024
Revised: August 12, 2024
Accepted: September 16, 2024
Published: September 21, 2024





In this regard, bioplastics, or biodegradable polymers, have been shown to be an intriguing and promising solution. However, to fully demonstrate the socioeconomic benefits of bioplastics and to further challenge the status quo of conventional petroleum-based plastics, ongoing innovation and global support are necessary. Polyhydroxyalkanoate (PHA), polycaprolactone, and polylactic acid (PLA) are some of the commercially available biodegradable plastics which have already influenced the plastic industries and changed the direction of polymer advancements.⁷ Poly-(butylene adipate-co-terephthalate) (PBAT) is the most widely produced biodegradable polymer nowadays, which is commercialized as Ecoflex, Eastar Bio, and Wango. 8,9 With numerous applications in packaging, consumer durables, and agriculture, the PBAT market is predicted to grow from \$1.1 billion in 2020 to \$2.7 billion by 2030. Poly(ethylene terephthalate) (PET) is also a well-known polyester with outstanding barrier and mechanical properties but has been questioned due to environmental concerns. Nevertheless, PBAT or PET are petroleum-based polyesters that produce hazardous and nonconsumable monomers after decomposition, especially terephthalic acid (TPA).

Considering this, 2,5-furan dicarboxylic acid (FDCA) is highly advocated as a renewable substitute for fossil-derived TPA in polyester synthesis. 12–14 The US Department of Energy in 2004 listed FDCA as one of the top 12 biobased platform chemicals to play an important role in establishing a sustainable future in the plastics or packaging industries.¹ Polyesters based on furan offer a class of bioplastics with great promise.¹⁶ Several chemical companies like BASF, ADM, Avantium, and DuPont are involved in the industrial production of FDCA (structural similarity to TPA) and FDCA-based polyesters, considering their potential application to packaging sectors to replace the widely used petro-based PET products.^{17–19} Numerous investigations have demonstrated the better thermal, mechanical, and gas barrier qualities of poly(ethylene 2,5-furanoate) (PEF), the polyester made from 2,5-FDCA and ethylene glycol, over that of its terephthalate counterpart, PET. 20,21 It is important to note that these exceptional qualities provide several benefits, particularly in packaging or bottle applications where strong heat resistance and a lower melting temperature are required, which facilitates the extrusion and blow molding processes. 21,22

Nevertheless, many research articles on furan-based polyesters have been published, including the synthesis, thermal, mechanical, barrier, and enzymatic degradation aspects, as well as crystallization kinetics. There are few comparative reports on PBAT and poly(butylene adipate-cofuranoate) (PBAF) polyesters, where biobased FDCA has been an effective substitute for TPA.²⁷ Biobased PBAF demonstrated better biodegradability and mechanical strength compared to petroleum-based PBAT. 27,28 Many studies on furan-based polyesters containing different glycol subunits or dicarboxylic acids as comonomers are also reported to supplement the drawbacks in the properties of PEF or PBAF. 24,29-31 Zubkiewicz et al. fabricated a series of novel and 100% biobased high-molecular-weight random aliphaticaromatic copolyesters comprising different amounts of sebacic acid and FDCA ester by eco-friendly melt polycondensation. The copolymer showed outstanding gas barrier properties to O2 and CO2 and can compete with currently available biodegradable Ecoflex polymer in several applications.³ Bikiaris and his co-workers reported a plethora of polyester from FDCA and its analogs, revealing the enormous interest in designing green plastics, both from a scientific and industrial perspective. ^{33–38}

Thermoplastic poly(ether-ester) elastomers (TPEEs), combining the benefits of thermoplastics and rubbers, are also constructed from biobased FDCA with high thermal resistance and elastic recovery properties. The renewable FDCA serves as a crystallizable hard segment in the multiblock copolymers, contributing to the high mechanical strength of TPEs.³⁹ FDCA-derived poly(1,4-cyclohexanedimethylene furandicarboxylate)-poly(tetramethylene glycol) TPEEs with controlled composition of soft and hard segments displayed good shape recovery as high as 84.9% at 200% strain and high melting point (Tm up to 198 °C), thus opening new avenues to design tailor-made TPEE with required properties. 40 A new type of segmented FDCA polyester incorporating the polysulfone moiety was also fabricated, demonstrating impressive tensile properties, excellent transparency, and solvent resistance, making it appropriate for uses like food and beverage packaging materials.⁴¹ However, the basic and relative understanding of the structural role of FDCA directly with TPA within the polymer chain and its influences on the biodegradation process is important to confirm its expanding applications. FDCA-derived polyester's distinct structure allows for the customization of its physicochemical characteristics to suit a broad range of applications. Moreover, its natural biodegradability makes it a sustainable replacement for more traditional materials.

To accomplish this, a series of FDCA-based copolyesters with favorable properties were synthesized from renewable feedstocks, dimethyl 2,5-furandicarboxylate (DMF), dimethyl sebacate (DMS), and 1,4-butane diol (BDO) or 1,5-pentane diol (PDO) as the glycols via a simple transesterification and polycondensation method, aiming to adhere our synthesis procedure with sustainability standards. The study's main premise is that the polymer's aliphatic polyester part will contribute to its good biodegradability, while the aromatic polyester portion will give it excellent mechanical and thermal qualities. Together, these monomers would create a linear macromolecular structure to preserve the necessary flexibility and processability as well as a reduction in the topological regularity of the macromolecule chain to inhibit crystallization. The impacts of compositions on the chemical structures, thermal, mechanical, and crystalline properties of the synthesized poly(butylene sebacate-co-furanoate) (PBSF) and poly(pentylene sebacate-co-furanoate) (PPeSF) copolyesters in comparison to their terephthalate counterparts are systematically investigated. The synthesized furanoate copolyesters exhibited good mechanical strength, high extensibility, and excellent shape recovery after stretching. The molecular weight and odd-even-numbered glycol units (BDO or PDO) in the polymer composition play a crucial role in the determination of complex viscosities and the shear modulus of copolyesters with applied shear. Furthermore, the biodegradation behavior of the copolyester exhibited good hydrolytic degradability to different extents in both chemical and enzymatic mediums, providing a more eco-friendly end-of-life option. The above findings show how structure and attributes relate to one another and offer a gentle method for creating high molecular weight furan-based polyester with potential uses to mitigate plastic pollution with eco-friendly alternatives.

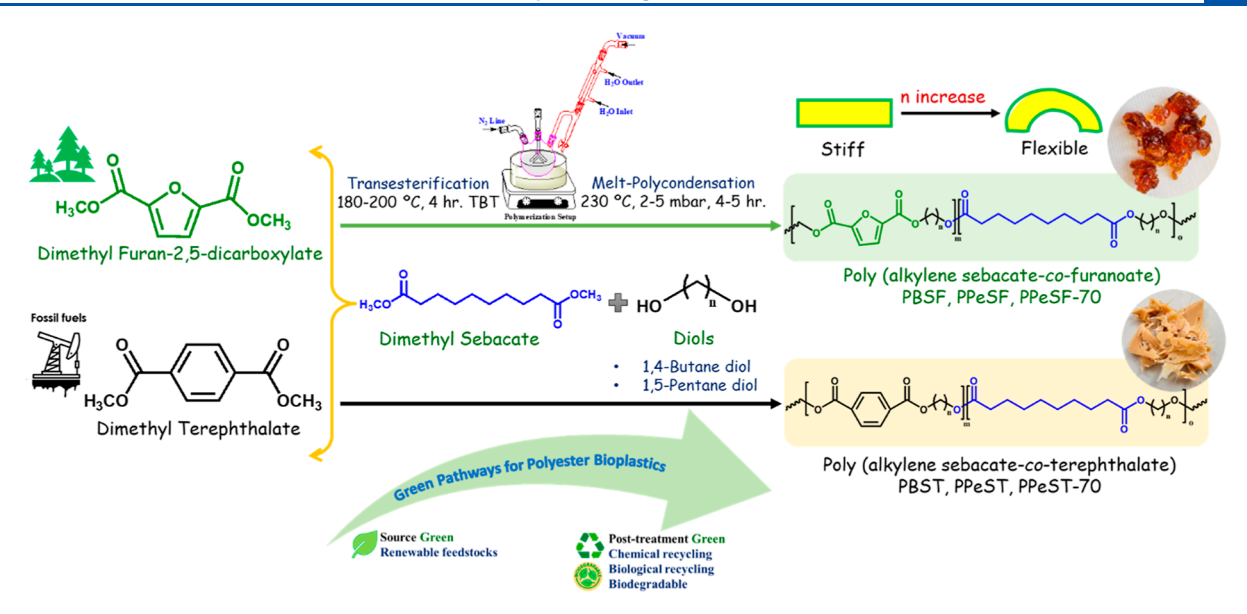
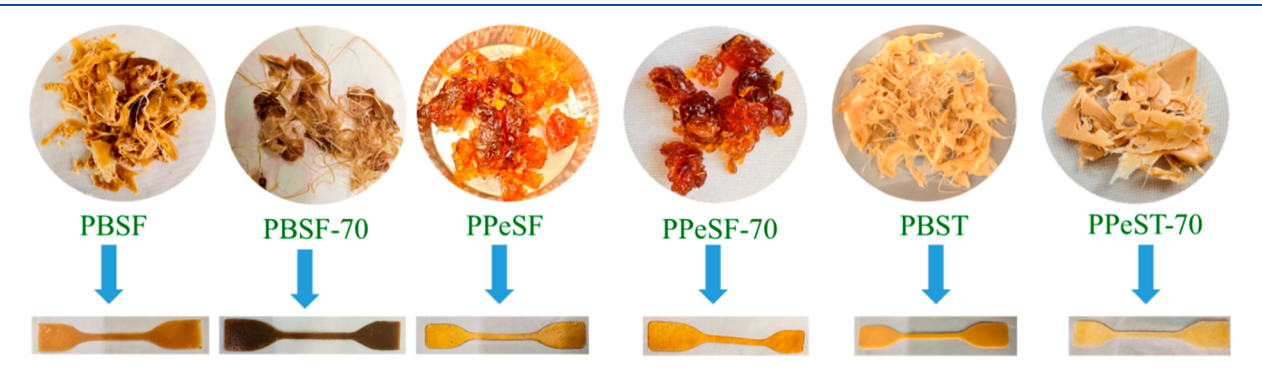


Figure 1. Schematic showing the fabrication of furan-based polyester and its terephthalate counterparts.

Table 1. Compositions and Characteristics of Furan-Based Co-polyesters^a

sample	feed ratio (mole) Aro.:Ali.:Diol	feed ratio (mol %) ^b Aro./Ali	yield (%)	intrinsic viscosity c [η] (dL/g)	$M_{\rm w} ({\rm g/mol})^d$	$M_{\rm w}$ (g/mol)(from GPC)
PBSF	0.5:0.5:1.5	51.8/48.2	75.6	0.670	43,790	39,360
PBSF-70	0.7:0.3:1.5	67.4/32.6	76.4	0.746	51,300	56,810
PPeSF	0.5:0.5:1.5	52.1/47.9	72.3	0.870	64,300	49,320
PPeSF-70	0.7:0.3:1.5	65.3/34.7	73.8	1.074	74,150	53,220
PBST	0.5:0.5:1.5	50.5/49.5	71.3	0.672	43,960	45,780
PPeST	0.5:0.5:1.5	51.6/48.4	74.9	0.847	61,780	53,620
PPEST-70	0.7:0.3:1.5	72.3/27.7	70.3	0.952	69,980	53,240

^aReaction conditions—transesterification: 180–200 °C for 4 h; polycondensation: 230–240 °C for 4–5 h. Aro. represents DMF/DMT, and Ali. is DMS. ^bMolar composition of aromatic and aliphatic diacid monomers from NMR. ^cIntrinsic viscosity values reported using the Billmeyer equation. $^{d}M_{w}$: weight-average molecular weight from viscosity.



Dumbbell-shaped Specimens

Figure 2. Pictures of some representative synthesized furan-derived polyester samples.

2. EXPERIMENTAL SECTION

2.1. Materials. Dimethyl furan-2,5-dicarboxylate (DMF, 98%) was purchased from Synthonix, Inc. (USA). Dimethyl terephthalate (DMT, 99%) was purchased from Sigma-Aldrich (USA). DMS (99%), BDO (99.5%), PDO (98%), and titanium(IV) butoxide (TBT, 97%) were procured from Fisher Scientific Chemicals (USA). Phenol (99+%) and 1,1,2,2-tetrachloroethane (98+%), utilized as a mixture for intrinsic viscosity measurements, were purchased from Thermo Scientific Chemicals, USA. All the other chemicals and solvents were used as received.

2.2. Synthesis of Poly(alkylene sebacate-co-furanoate) (PBSF and PPeSF). Furan-based copolyesters were synthesized by a traditional two-step melt polymerization procedure involving transesterification and polycondensation, as shown in Figure 1. PBSF and PPeSF polyesters were prepared from different molar ratios of dimethyl furandicarboxylic acid, DMS, and 1,4-butanediol or PDO. The sample codes, reaction conditions, and relevant data are presented in Table 1 later. In the typical polymerization process, the diesters (DMF and DMS), diols (BDO or PDO), and catalyst TBT (0.1 wt % of total diesters) were charged into a 250 mL reaction flask equipped with a mechanical stirrer, N₂ line, and a condenser.

The molar ratio of -COOR to -OH was kept at 1:1.5. The transesterification reaction was carried out at 180 °C for 1.0 h, and then the temperature was gradually increased up to 190-200 °C for 2.0-3.0 h under a nitrogen atmosphere. After successfully collecting 90-95% of the theoretical amount of byproduct, i.e., methanol, a vacuum was applied to initiate the polycondensation process. Subsequently, the temperature was increased to 230-240 °C, and the reaction was kept under a vacuum at 2.5-3.0 bar pressure for 4-5 h to complete the polymerization. The second stage was finished at the moment when low-speed stirring revealed the Weissenberg effect. 42-44 Subsequently, the resultant polymer was removed from the flask right away and allowed to dry for 24 h at room temperature. The obtained polymers resembled filamentous rubbery nature with a yellowish-brown color, as shown in Figure 2. Copolyesters, poly-(butylene sebacate-co-furanoate) and poly(pentylene sebacate-cofuranoate), are labeled PBSF and PPeSF, respectively, and are characterized without further purification. PPeSF-70 is a polymer consisting of only 70 mol % of DMF and 30 mol % of DMS and PDO. Terephthalate-based equivalent copolyesters (PBST, PPeST, and PPeST-70) were also similarly synthesized following the polymerization process to compare with furanoate-derived copolyesters.

2.3. Characterization. The synthetic polymers' molecular structure was determined by employing Fourier-transform infrared spectroscopy (FTIR, PerkinElmer 200). Attenuated total reflectance mode in the wavenumber range of 4000–500 cm⁻¹ (resolution of 8 cm⁻¹) with 32 scans per sample were followed.

To describe the compositions of polymers, 1H NMR spectra of the polyesters were obtained using a Bruker Advance-III 300 MHz spectrometer with deuterated chloroform (CDCl3) as the solvent and traces of tetramethylsilane as an internal reference. The chemical shift (δ) was stated in parts per million (ppm). The sample concentration is about 20 mg/mL, and the spectra were recorded at room temperature.

The intrinsic viscosities (η) of the polyesters were measured at 20–25 °C using a Ubbelohde viscometer (CANNON 50 L487). The samples at a concentration of 0.5 g/dL were dissolved in a 60/40 w/w solution of phenol/1,1,2,2-tetrachloroethane,, and their flow time was measured using the viscometer. The $[\eta]$ value of each sample was calculated following both the Billmeyer and Solomon-Ciuta relationship

Billmeyer equation:
$$[\eta] = 0.25(\eta_r - 1 + 3\ln \eta_r)/C$$
 (1)

where c is the solution concentration, t is the average flow time of the polymer solution, and $t_{\rm o}$ is the average flow time of the solvent. $\eta_{\rm r}$ represents the relative viscosity, i.e., $t/t_{\rm o}$. The reported viscosity values are the average of three measurements to ensure the accuracy.

The number-average $(M_{\rm n})$ and weight-average $(M_{\rm w})$ molecular weight of the PEF polyester samples was calculated from the obtained intrinsic viscosity $[\eta]$ values using the following relation for PET in 60/40 phenol/1,1,2,2-tetrachloroethane at 25 °C, as mentioned in the earlier reported literature

$$\eta = 3.72 \times 10^{-4} (M_{\rm n})^{0.73}$$

$$\eta = 4.68 \times 10^{-4} (M_w)^{0.68}$$

Gel-permeation chromatography (GPC) was used to determine the molecular weights of the synthesized polyesters using a 1525 binary HPLC pump (Waters, MA) equipped with 5 μ m phenogel columns and tetrahydrofuran as the eluent solvent (flow rate of 1 mL/min) at 30 °C. The calibration curve was obtained using polystyrene standards

DSC (TA Instruments, Q100, USA) was used to examine the thermal properties of the synthesized copolyesters under a N_2 atmosphere. Approximately 8–10 mg of polymeric material were typically heated in steps of 10 °C/min, commencing from -70 °C and ending at 200 °C (first heating), chilled to -70 °C (cooling scan) at a rate of 10 °C/min, and then reheated to 200 °C (second heating) at a scanning rate of 10 °C/min. Glass transition temperature (T_g) and

melting temperature $(T_{\rm m})$ were calculated from the second heating scan. The data was analyzed using TA Universal Analysis software.

Thermal stabilities of synthesized polyesters were measured between 30 and 600 °C using a thermal gravimetric analyzer (TA Instruments 550 Discovery Series) at a constant heating rate of 10 °C/min under nitrogen flow. The derivative thermogram plot was used to determine the temperature corresponding to the first weight loss ($T_{\rm onset}$) and the highest weight loss temperature ($T_{\rm max}$).

The rheological properties of the polyesters were characterized by a Netzsch Kinexus Prime *pro+* rotational rheometer with a 25 mm diameter parallel plate and 0.5 mm gap. An oscillation frequency sweep was performed at 160 °C with angular frequency varying from 0.1 to 150 rad/s and a controlled strain of 1.5%. An oscillatory temperature ramp at an angular frequency of 1 Hz and a shear strain of 1.0%, beginning from 25 to 150 °C at a rate of 3 °C min⁻¹ were performed.

XRD patterns were recorded with a Lab X Shimadzu XRD-6100 using Cu K α radiation (λ = 0.154 nm), working at a tube current of 30 mA and an operating voltage of 40 kV. The scanning was from 5° to 60° at a speed of 1°/min, and the preset time was set as 1.20 s.

The synthesized copolyesters were hot-pressed at 180 °C for 5 min (3 tons/m² pressure) using a laboratory press (Carver Autoseries Plus) to prepare thick films of approximately 1.0–1.2 mm thickness for mechanical testing.

Stress—strain measurements were performed by a universal testing machine (UTM, Schimadzu, AUTOGRAPH AGX-V) equipped with a 10,000 N load cell. Dumbbell-shaped specimens of a 1.0 mm specific thickness (gauge length of 35 mm) were cut from the molded films following the ASTM D412 standard. The crosshead speed was kept at 100 mm/min, and an average of three test samples were reported for tensile strength (TS) values.

The polyester samples' dynamic mechanical characteristics were examined using a TA Instruments Q800 DMA in the temperature range of -60 to 100 °C at a heating rate of 3 °C min⁻¹. Every measurement was performed in the tension mode at a 1 Hz frequency and $20~\mu m$ strain amplitude.

2.4. Enzymatic and Chemical Degradation Tests. Enzymatic degradation was executed in a 0.1 M phosphate buffer solution of pH 7.0 using the lipase enzyme from *Candida rugosa*. Chemical degradation was performed in a 1 M NaOH aqueous solution of pH 13–14. For each case, the specimen thickness (1.0-1.2 mm) and weight were taken fixed at 0.09 ± 0.01 g. The sample was put inside a vial (10 mL) at 37 °C and kept for 1 month of analysis and checked over 1 week intervals. To ensure the highest level of enzyme activity during the enzymatic breakdown, the medium was replaced daily. The degradation rate was analyzed by initial and final weight loss and the structural changes by FT-IR spectroscopy. The biodegradability of polymer samples via surface phenomenon was examined by scanning electron microscopy imaging.

3. RESULTS AND DISCUSSION

3.1. Preparation of Aliphatic-Aromatic Copolyesters.

Furan-based high molecular weight copolyesters were synthesized by a conventional two-step growth polycondensation technique from biomass-derived monomers such as DMF, DMS, and different aliphatic diols (BDO or PDO). Petrochemical-based DMT-derived copolyesters were also prepared for comparison study. Because of its structural advantages, biomass-based DMF is an excellent alternative to fabricating sustainable polyester films and will offer superior elastic recoveries while still being biodegradable. The central hypothesis of this study is centered around the primary idea that the aliphatic polyester part will contribute to the polymer's biodegradability, and the aromatic polyester portion will offer good mechanical and thermal qualities of the polymer. The polymerization reaction conditions, conversion, intrinsic viscosity, molecular weights, and dispersity (D) of all of the resulting copolyesters are summarized in Table 1. The molar

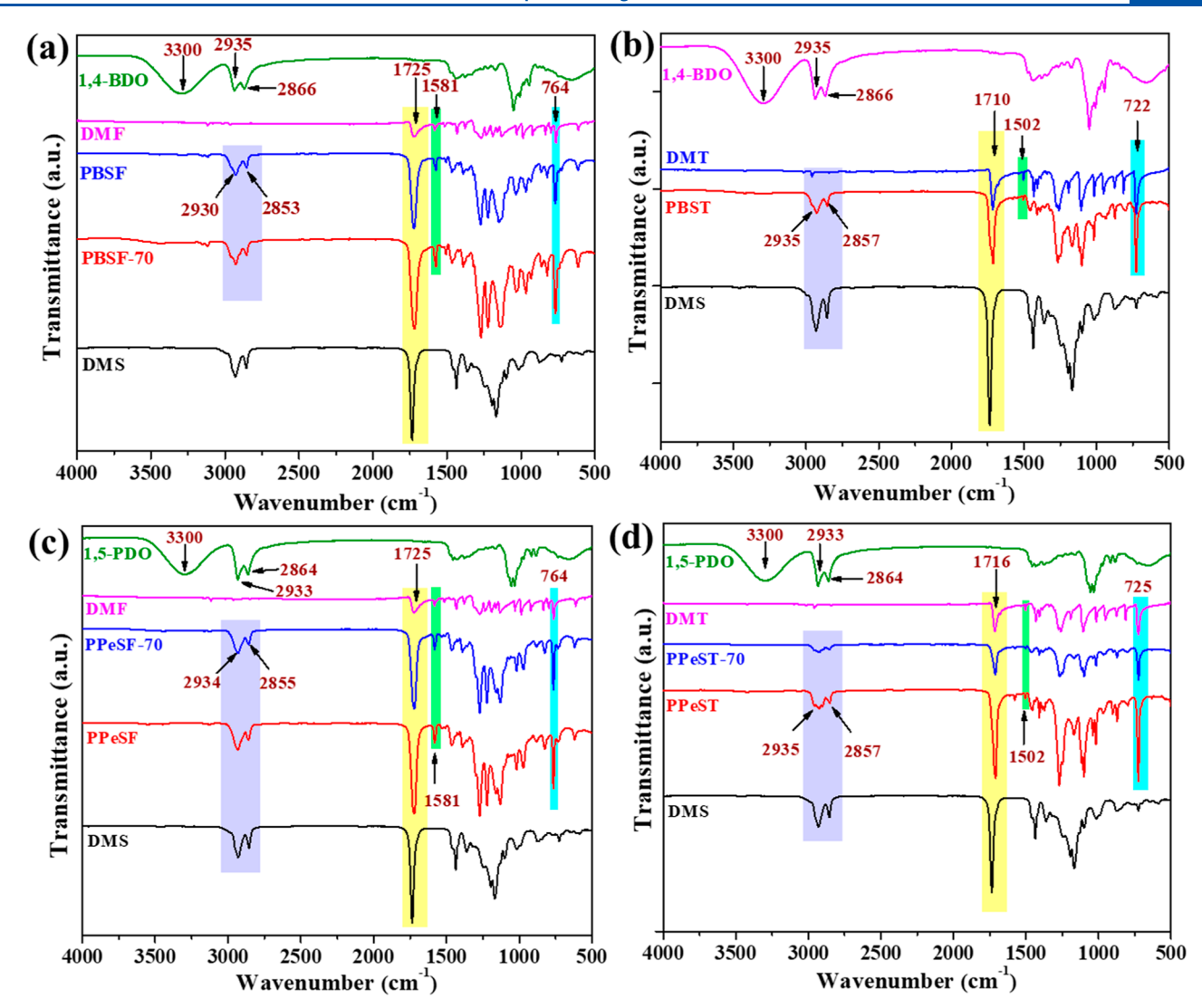


Figure 3. FTIR spectra of (a) PBSF and PBSF-70, (b) PBST, and (c,d) PDO-derived copolyesters along with the reacting monomers.

ratio of the diol (-OH) to the ester (-COOR) group is kept at 1.5 to ensure complete consumption of the diester moiety. To guarantee the different reactivities of the aromatic and aliphatic diesters (DMF and DMS), the ester-exchange reaction temperature was monitored over a temperature range of 170–200 °C. Finally, to facilitate the removal of byproducts (excess diols) by decreasing the viscosity of the polymer melts, the temperature was raised to 240 °C for polycondensation, resulting in the formation of high molecular weight copolyesters. High temperatures (>240 °C) and extended reaction times cause degradation of polymer chains and generate carboxyl groups, hence not favored. 45,46 The copolyesters produced are random copolymers despite distinct ester-exchange steps.

The $[\eta]$ values of all of the polyester samples ranged from 0.67 to 1.09 dL/g. The molecular weights $(M_{\rm n})$ of the polyester generated from furans were obtained between 39,300 and 56,800 g/mol, which indicates that the polymers' mechanical strength and elasticity are adequate and are roughly within the range of commercial industrial polyester PBAT standards. Evidently, $M_{\rm w}$ increases with the increase in the diol chain length.

The polymers discharged from the reactor were slightly colored with a filamentous rubbery nature. All of the samples

are not transparent and brown, except for PBST and PPeST-70, which are slightly off-white and opaque (Figure 2). For additional mechanical and rheological examination, all of the polymers have been effectively processed into free-standing thick films with consistent thicknesses of around 1.0–1.2 mm.

3.2. Structural Characterization of Copolyesters. FTIR and ¹H NMR spectra of furanoate and terephthalate polyesters with different monomer feed ratios are recorded to determine the functional groups present in a polymer. Figure 3a,b shows the representative FT-IR spectra of PBSF and its terephthalate counterpart PBST along with the reacting monomers, respectively. The absorption peak at around 3300 cm⁻¹ is ascribed to the -OH stretching vibration in the diols, which vanishes after the successful formation of the polymer. The C-H antisymmetric and symmetric stretching vibrations of methylene groups were observed at 2935 and 2866 cm⁻¹, which remain in the polymer. The intense peak at 1725 cm⁻¹ is assigned to the stretching vibration of the ester carbonyl group (-C=O). The presence of characteristic peaks in PBSF assigned to the furan ring, including C=C ring stretching vibrations at 1581 cm⁻¹, =C-O-C= absorption frequency at 1025 cm⁻¹, and the furan ring vibration signature peak at 764 cm⁻¹, confirms successful copolymerization. Moreover, the fingerprint region peaks for PBST appear at 1502 cm⁻¹ due to

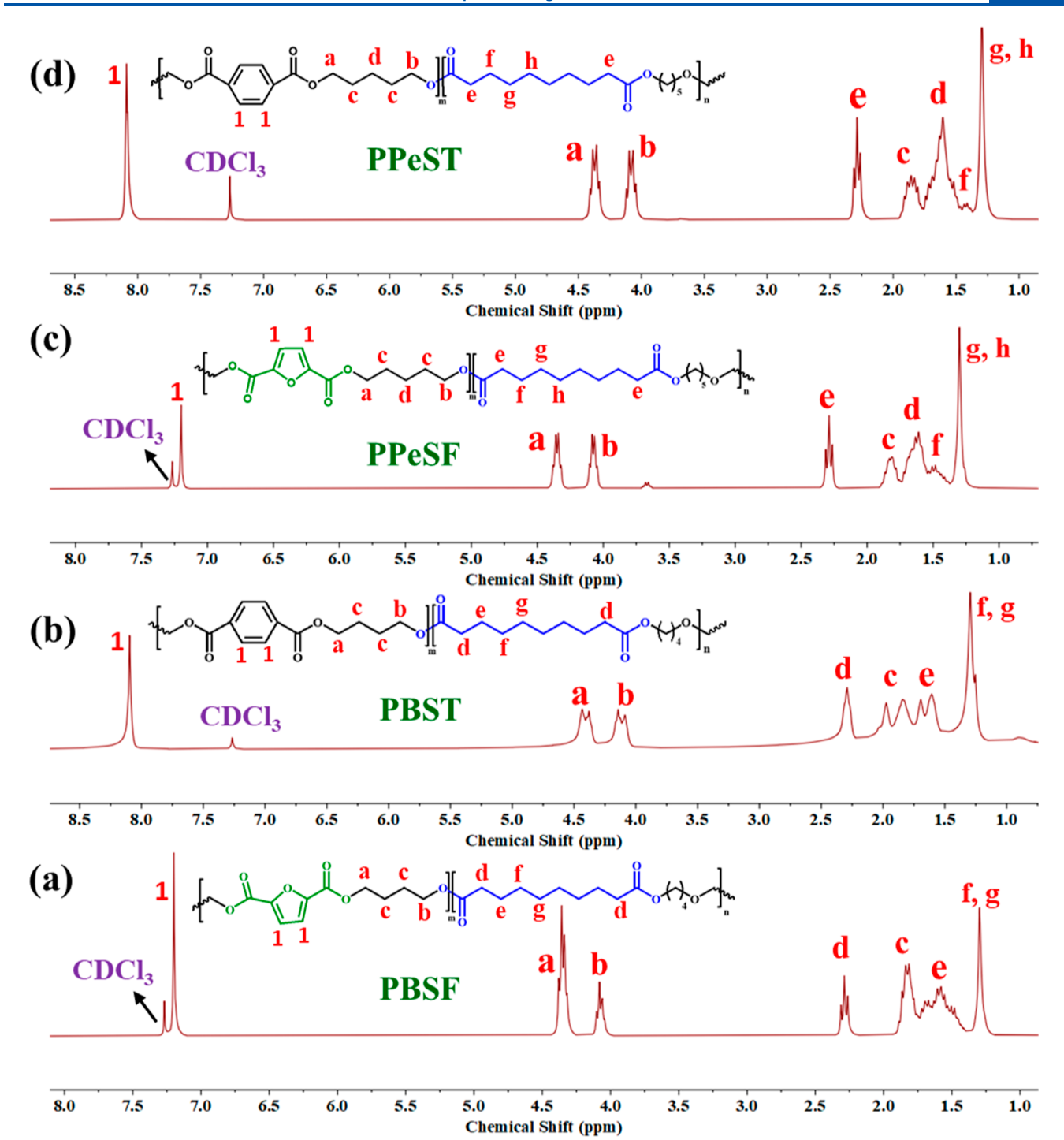


Figure 4. ¹H NMR spectra and characteristic peak assignments of (a) PBSF, (b) PBST, (c) PPeSF, and (d) PPeST.

benzene ring -C=C- stretching, and 722 cm⁻¹ is assigned for the aromatic ring vibration. The spectral assignments for the PPeSF, PPeSF-70, PPeST, and PPeST-70 samples are also provided in Figure 3c,d. Results from FT-IR analysis suggested that both aliphatic and aromatic components were successfully incorporated as a part of the preparation of a furan-based high molecular weight copolyester.

The molecular structures of PBSF, PPeSF, PBST, and PPeST were also confirmed using ¹H NMR spectroscopy, and the peak assignments to their respective protons are shown in Figure 4a—d. In the case of PBSF, the furan ring heterocyclic proton (—CH, 1) chemical shift appears at 7.20 ppm. Signals at

4.30 and 4.10 ppm are assigned to the methylene protons $(-CH_2)$, a, and b) connected by ester bonds of the DMF and DMS units. These hydrogen atoms are adjacent to the -OCO-moiety and are more deshielded, thus appearing in the downfield region. The chemical shift of $-CH_2$ (d) adjacent to the ester carbonyl group of the DMS unit appears as a triplet at around 2.30 ppm. The $-CH_2$ proton signals from BD (c) appear at around 1.81 ppm. A broad multiplet peak in the range 1.5–1.6 ppm is ascribed to the symmetrical $-CH_2$ units (e) from the DMS unit. The resonances at 1.30 ppm correspond to the methylene protons of the aliphatic DMS units. Moreover, for the PBST polyester, the aromatic ring

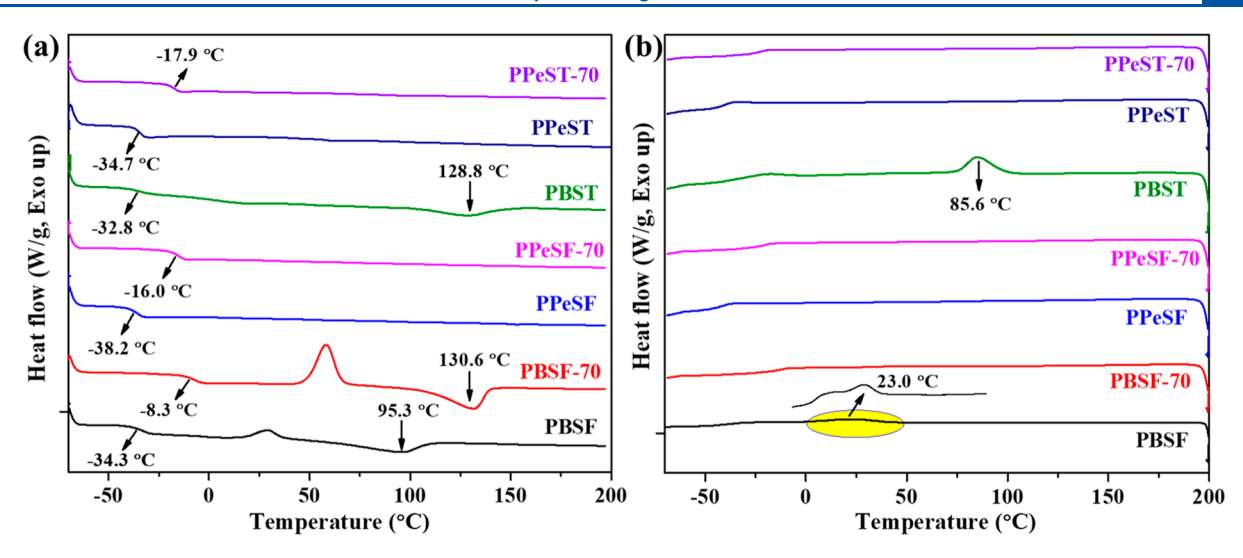


Figure 5. DSC thermograms of furanoate-based and terephthalate-based copolyesters (a) heating scan and (b) cooling scan.

proton (-CH, 1) appears in the more downfield region at 8.10 ppm. The resonances related to methylene protons ($-CH_2$) appear in the same region as that for the furan polyester.

Figure 4c,d represents the NMR spectra of PDO-derived furanoate and terephthalate polyester. Similarly, the heterocyclic protons of the furan ring in PPeSF and the benzene ring proton in PPeST appear at 7.20 and 8.15 ppm, respectively. The proton signals relative to methylene units appear at similar chemical shifts, revealing the formation of copolyesters. The spectral assignments for the PPeSF-70 and PPeST-70 copolyesters are identical with the above PDO-derived polymers. Therefore, all of the copolyesters synthesized showed the expected resonances for each of the DMF, DMS, and BDO or PeDO components, favoring the polymerization process.

3.3. Thermal Characterization of Polyester Films. The synthesized polyesters were subjected to DSC analysis to record the thermal transitions at different temperatures. Figure 5a,b depicts the heating and cooling DSC thermograms of the copolyesters with varying compositions. PBSF exhibited a glass transition temperature $(T_{\rm g})$ of -34.3 °C and a melting temperature $(T_{\rm m})$ of 95.3 °C. Whereas, PBST registered a $T_{\rm g}$ of -32.8 °C and a $T_{\rm m}$ of 128.8 °C, respectively. With increasing furan content, i.e., for PBSF-70, the $T_{\rm g}$ increased to -8.3 °C, and $T_{\rm m}$ of 130.6 °C was observed. The presence of symmetrical or planar TPA moiety infers efficient molecular packing, resulting in increased T_{m} . From the cooling scan, PBST shows a prominent crystallization (T_c) peak at 85.6 °C, while the crystallization of PBSF occurs slowly (around 23.0 °C), indicating weak crystallinity. The distinct crystallizabilities of FDCA and TPA can be used to determine the structural differences between the two copolyesters. As anticipated from the observation, the favorable π – π stacking of the phenyl rings in DMT leads to quick crystallization, whereas kinked conformation and poorly packed furan rings in DMF cause a somewhat slow crystallization process.²⁷ On the other hand, all the PDO-derived copolyesters exhibited one glass transition temperature, and no melting endotherms were observed. PPeSF and PPeST presented $T_{\rm g}$ of -38.2 and -34.7 °C, respectively. With an increase in the DMF & DMT content, PPeSF-70 and PPeST-70 showed a drastic increase in the T_{g} values to -16 and -17.9 °C (Figure 5a), respectively. Furthermore, the absence of a $T_{\rm m}$ indicates that DMF or

DMS uniform repetitions (crystal structures) are effectively inhibited by the odd-number carbon effect of PDO. About $T_{\rm g}$ or $T_{\rm m}$, the furan-based polyester samples showed lower values than their terephthalic counterparts, even though both polymer families exhibit the same odd—even pattern. A different balance of the key structural features (symmetry, bond angles, ring aromaticity, etc.) between the two families results in less efficient crystal packing in furanoate-derived polyesters.

The thermal stability of copolyesters was accessed through thermogravimetric analysis (TGA) in an inert environment. The thermal decomposition curves and temperatures corresponding to 5% and 50% weight loss are reported in Figure 6.

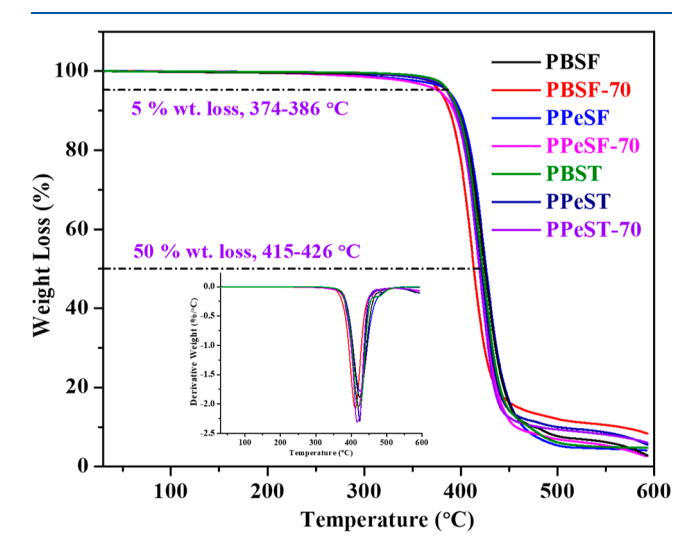


Figure 6. TGA of furanoate-based and terephthalate-based copolyesters.

The initial thermal decomposition temperature at 5% weight loss ($T_{5\%}$) for all the fabricated copolyesters ranged from 374 to 386 °C. Despite being solely biomass-based, TGA revealed an average maximum degradation temperature ($T_{50\%}$) ranging from 415 to 426 °C, highlighting the furan-derived samples' reliable thermal stability for various applications. Additionally, the DTG curves (inset) of all of the polyesters showed a single peak, and the initial and maximum degradation temperatures

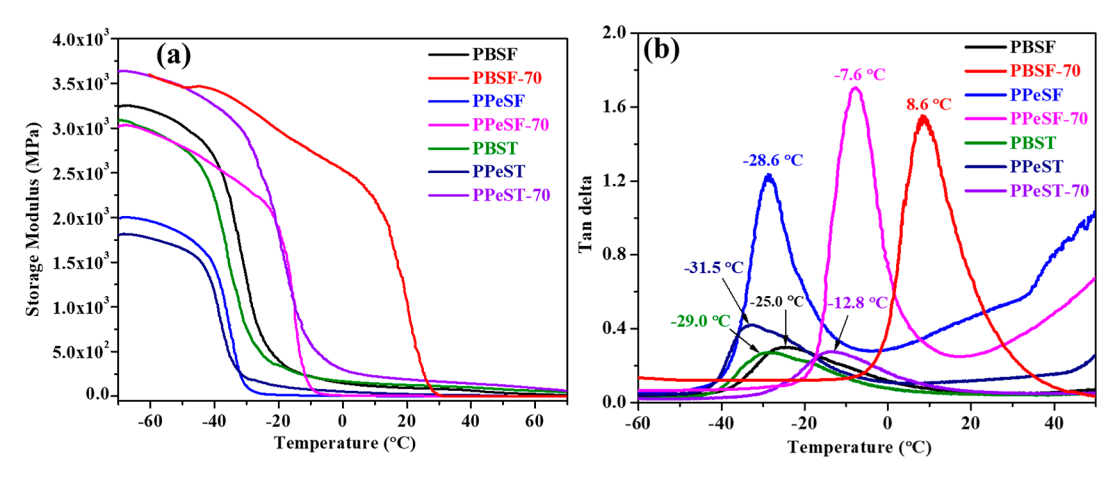


Figure 7. Temperature dependence of (a) storage modulus (E') and (b) loss factor (tan δ) for the furanoate-based and terephthalate-based copolyesters.

Table 2. Thermal Transition Parameters of the Furan-Derived Polyesters

sample	$T_{\rm g}$ (from DSC) (°C)	$T_{\rm g}$ (from tan δ) (°C)	E' @ 25 °C (MPa)	Young's modulus (MPa)	TS (MPa)	elongation at break (%)	crystallinity $(X_c, \%)$ (from XRD)
PBSF	-34.0	-25.0	88.10	0.32	8.40	617	10.2
PBSF-70	-8.3	8.6	230.0	0.60	10.72	325	13.7
PBST	-33.0	-29.0	119.40	0.34	8.31	497	19.2
PPeSF	-38.0	-28.6	1.95	0.31	6.40	70	4.3
PPeST	-34.0	-31.5	20.98	0.41	7.32	160	6.8
PPeSF-70	-16.0	-7.6	4.12	0.47	6.82	584	9.1
PPeST-70	-17.0	-12.8	177.10	0.37	6.10	268	9.6
PBAT	NA	-20.0		91.1	49.7	876	

fell within a restricted range, suggesting a comparable random copolymer structure. The thermal decomposition patterns of PBST and PPeST were consistent with other furan polyesters, including poly(butylene succinate-co-butylene furan dicarboxylate) and poly(alkylene adipate-co-furanoate). Moreover, based on the TGA results, all of the polyesters' thermal breakdown temperatures are higher than 400 °C, which distinguishes them from commercially available biodegradable polyesters such as PLA or PHAs.

The thermo-mechanical behavior of the copolyesters at different molar compositions was investigated using DMA measurements in the tensile mode. Figure 7 shows the temperature dependence plot of storage modulus (E') and tan δ for the polyester films. All of the furan-based polyester exhibited a lower room-temperature (25 °C) tensile storage modulus in comparison to its terephthalate-derived equivalent, as tabulated in Table 2. Storage moduli decreased with increasing diol chain length, which is attributed to increased flexibility in the polyesters. The peak temperature of the tan δ curve indicates the T_g value of each polymer. PBSF, PBSF-70, PPeSF, and PPeSF-70 registered $T_{\rm g}$ values of -29.0, 8.6, -28.6, and -7.6 °C, respectively, whereas their terephthalate counterparts PBST, PPeST, and PPeST-70 exhibited T_g values of -25.0, -31.5, and -12.8 °C, respectively. The glass transition temperature was found to gradually increase as the FDCA level in the polymer composition increased, consistent with the patterns seen in the DSC analyses. Furthermore, the peak intensity (i.e., the tan δ value) of furanoate-derived polyester is higher than terephthalate counterparts (0.27 vs 0.30) (0.41 vs 1.21) (0.27 vs 1.70). Theoretically, a polymer with a greater tan δ value will exhibit less solid-like properties because of the chains' increased segmental mobility. Thus, it

makes sense that the presence of asymmetric FDCA would support the polymer chain's favorable segmental movement and active conformational changes.²⁷

3.4. Mechanical Properties of Polyester Films. The mechanical performance of the compression-molded films was evaluated by uniaxial tensile testing. Figure 8a displays the stress-strain curves of copolyesters with different compositions, and the values of TS and strain at break are collected in Table 2. The mechanical aspects of PBSF, PPeSF, PPeSF-70, and their terephthalate counterparts were directly compared to interpret the effect of biobased FDCA in the BDO and PDOcontaining polymer systems. PBSF shows the highest TS of 8.40 MPa and outstanding elongation at a break (EAB) of 617%, which is similar to that of PBST (TS of 8.31 MPa and EAB of 497%). PBSF-70 exhibited the highest TS of 10.72 MPa. The chain flexibility (i.e., T_g value) and molecular weight are crucial to determining the mechanical response. PPeSF exhibited a TS of 6.40 MPa and an EAB of 70%, while PPeST yielded a higher TS of 7.32 MPa and a lower EAB of 160%. The dramatic decrease maintains the lateral packing of the aligned polymer chains and imparts rigidity in the polymer, giving greater stress with a corresponding reduction in the elongation at break.²⁸ In contrast to PBSF, the odd-even number effect of the diol enhances the overall elastic properties. The presence of an odd carbon-numbered PDO moiety in PPeSF disrupts the overall symmetry in the polymer and affects the linear stacking position in comparison to the even carbon-numbered butylene moiety BDO moiety in PBSF. However, the TS of PPeSF-70 increases with increasing aromatic content since a higher ring percentage results in a stiffer chain structure. PPeSF-70 (70 mol % DMF) has a high TS of 6.82 MPa and an EAB of 584%, while PPeSF-70 (70 mol

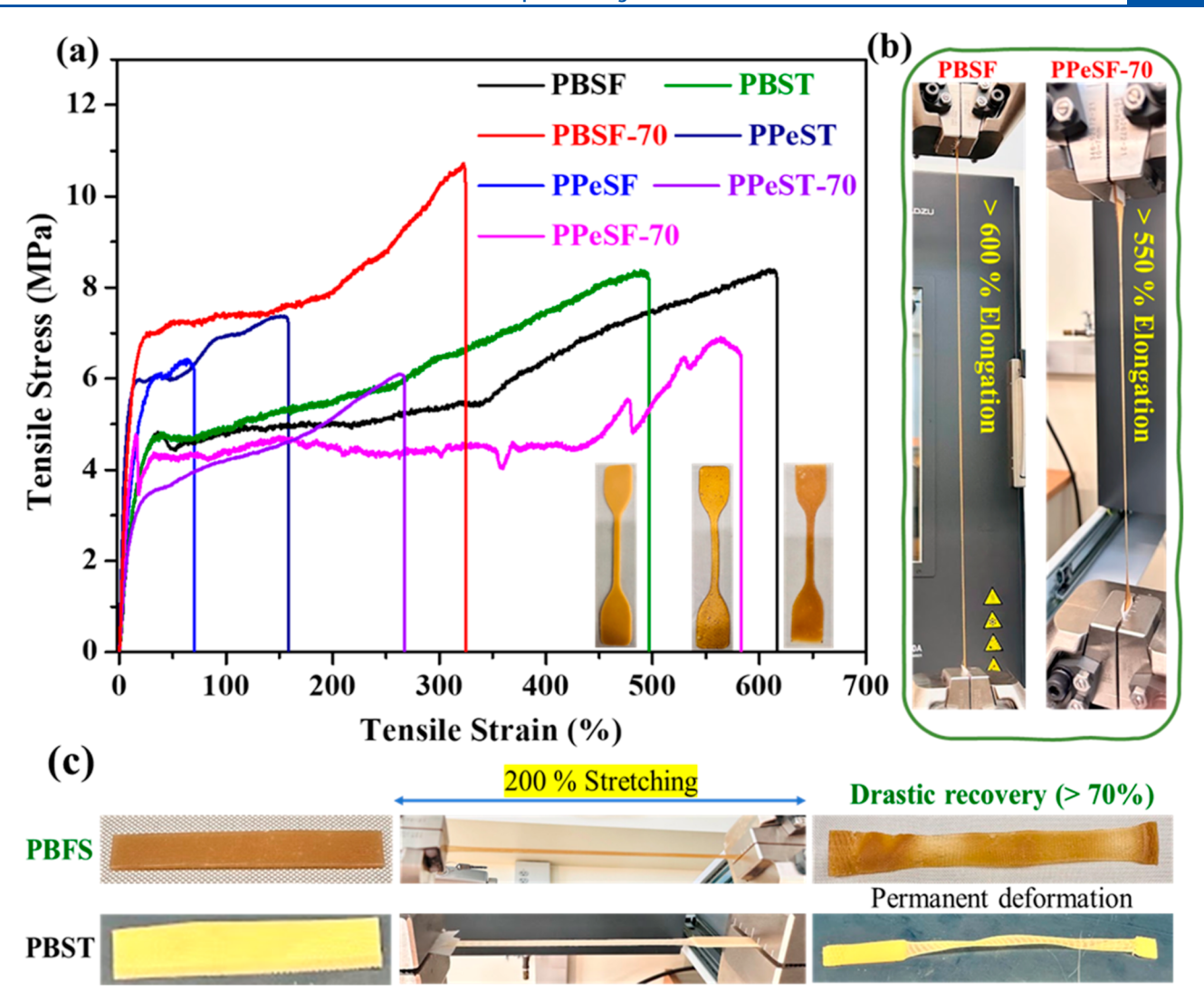


Figure 8. (a) Stress—strain measurement curve of the synthesized copolyesters. (b) Photographs showing extensive elongation of PBSF and PPeSF-70. (c) Illustration of the elastic recovery of PBSF and PBST.

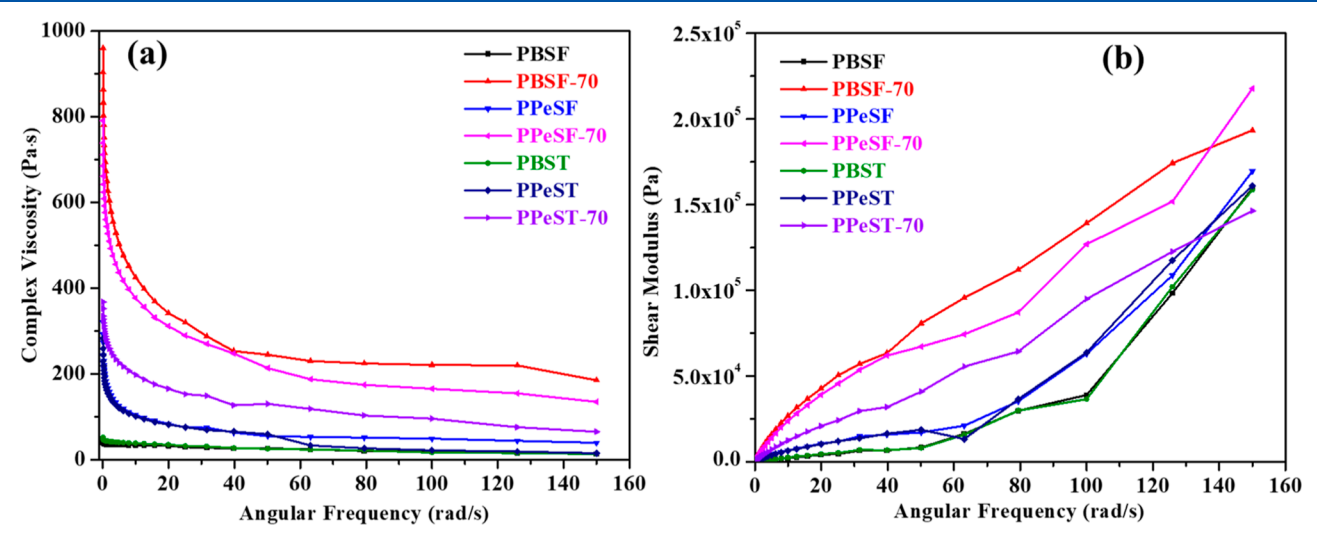


Figure 9. (a) Complex viscosity and (b) shear modulus of copolyesters as a function of angular frequency at 160 °C.

% DMT) yielded a TS of 6.10 MPa and a lower EAB of 268%. The TS of PPeSF-70 is analogous to that of its terephthalate

counterpart, as the molecular weights of the polymer are similar.

The elastic recovery of the synthesized PBSF versus PBST was visually compared in Figure 8c. After 200% stretching of the polyester films, there is an apparent distinction in the elastic recovery. Upon release, PBSF exhibited an instant 70% elastic recovery rate, whereas PBST demonstrated an irreversible deformation leading to a permanent loss in mechanical strength. The kinked and semirigid chain structure of furan-moiety enhances the spring-like motion and entropic recovery by breaking the symmetry or molecular packing of the polymer chain, resulting in an increased elastic recovery rate. Conversely, in PBST, the elastic restoration is disrupted by the presence of symmetric and rigid DMT units, which strengthens the molecular packing of the aligned chains. In light of this, PBSF is more durable than PBST over the long run.

3.5. Rheological Properties of Polyester Films. Figure 9a,b shows the complex viscosity and shear modulus as a function of the angular frequency of copolyesters at 160 °C. The viscoelasticity of polymers is predominantly determined by their chemical structure and molecular weight. 49 All the synthesized polyesters exhibited a linear decrease in viscosity with increasing applied angular frequency. Due to the low molecular weight, PBSF and PBST exhibited the lowest complex viscosity throughout the whole frequency range. Since entanglements grow with molecular weight, so does complex viscosity. PPeSF exhibited higher complex viscosity than PBSF due to its higher molecular weight. It is equally important to remember that PPeSF-70 has a higher complex viscosity (η^*) and storage modulus (G') than PPeST-70 throughout the observed frequency range. Among the six synthesized copolyesters composed of a mixture of odd/even moieties, PPeSF-70 exhibited the highest zero-shear viscosity, which indicates that the polymer structure is the stiffest in the absence of any applied shear.

Accordingly, the higher G' of PPeSF-70 to PBSF or PPeSF can be attributed to only a higher number of chain entanglements (Figure 9b). Theoretically, it is believed that the nonplanar and distorted DMF units are more effective than the rigid DMT at interdiffusing and entangling with the aliphatic sections.²⁷

3.6. Structural Characterization of Polyester. An XRD study was done to look into the microstructure of the furanbased polyesters with various glycolic subunit lengths. Figure 10 shows that PBSF and PBST have similar diffraction peaks at 11.9, 18.7, 21.3, 23.8, and 28.1°. The two peaks at 21.3 and 23.8° belong to the {110} and {010} planes, respectively, and the peak at 28.1° is allocated to the {120} plane. 50 The crystalline attributes at $2\theta = 18.7^{\circ}$ account for the formation of the monoclinic unit cell structure of the {020} plane. PBSF-70 exhibited crystalline diffraction patterns similar to those of the PBSF films. The inclusion of a 1,5-PDO unit in the PPeSF disrupts the regularity of the polymer chain sequence due to a possible "odd-even" effect, resulting in the PPeSF amorphous nature. This was evident that both PPeSF and PPeST displayed bell-shaped diffraction peaks with a very broad background, typical of an amorphous material. Meanwhile, the appearance of diffraction patterns in PPeSF-70 and PPeST-70 (70 mol % of DMF or DMT) were predominantly in the amorphous state except for PPeST-70, which exhibits intense diffraction peaks at 11.9°, indicating higher crystallinity in the material. These outcomes aligned with the findings of the DSC analysis. DSC thermographs of PPeSF and PPeSF-70 revealed the absence of melting and crystallization peaks, and only a vanishingly melting peak with low enthalpy is observed in

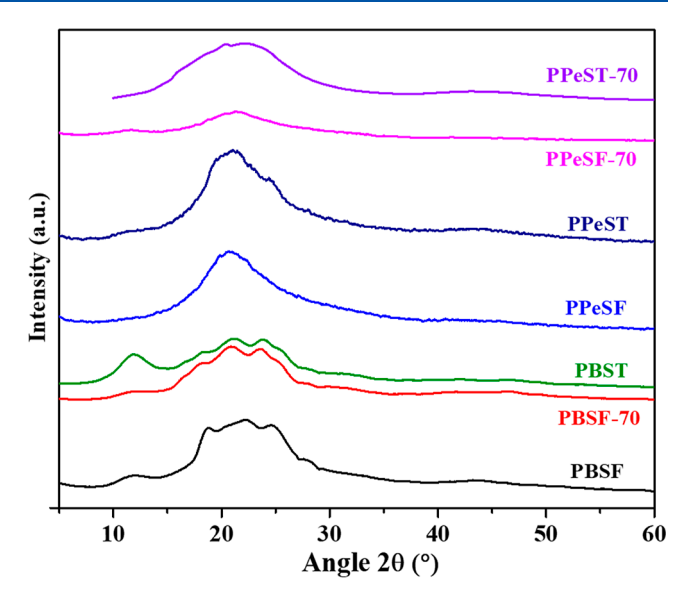


Figure 10. WAXS patterns of the compression-molded polyester films

PBSF or PBST. The crystallinity values calculated from WAXS are summarized in Table 2. An overall comparison contrasting the trends of furan-derived PBSF and PPeSF copolyesters suggests that PBSF samples with several intense peaks have larger crystal domains, indicating a semicrystalline nature.

3.7. Chemical and Enzymatic Degradation Studies. Finally, a preliminary biodegradation study of a representative polyester sample, PPeSF, was performed by treating the polymer films with the Lipases enzyme from C. rugosa for 30 days. The sample weight loss, chemical structural analysis, and surface morphology as a function of degradation days were recorded. In particular, film weight loss of the polymers was monitored over time, and the relative degradation percentage was calculated. The weight loss of the PPeSF film in the enzyme-free control sample was negligible (about 1.2%) after treatment in phosphate buffer for a month (data not shown). In the enzymatic solution, within 14 and 30 days, PPeSF was reduced to 15% and 35% of its initial weight. This is because the active site of lipase was the most accessible to the linear aliphatic sebacate chains along with asymmetric or distorted FDCA's intrinsic structural oddity in the polymer chain. Figure 11a shows the FTIR spectral changes of PPeSF films before and postdegradation, confirming the enzyme specificity. During the enzymatic breakdown, there were noticeable changes in the spectrum. With an increase in degradation time, the PPeSF carbonyl peak (C=O) intensity at 1720 cm⁻¹ dramatically reduced, while a new carbonyl peak from the hydrolyzed furanoate polyester emerged at about 1642 cm⁻¹ at the same time. Also, the peak intensity at 1575 cm $^{-1}$ (-C= C- stretching) and at 1224 and 1022 cm⁻¹ (C-O-C furan ring stretching vibration) increases, suggesting that FDCA's ester groups are susceptible to hydrolysis upon enzymatic breakdown.

To further investigate the enzymatic degradation phenomenon, the surface morphological changes were recorded, as displayed in Figure 11b. Enzyme specificity, which results from precisely docking the polymer chains into the enzyme's oriented active regions, initiates enzymatic hydrolysis. With the increase in degradation time, the enzyme attacks and eats

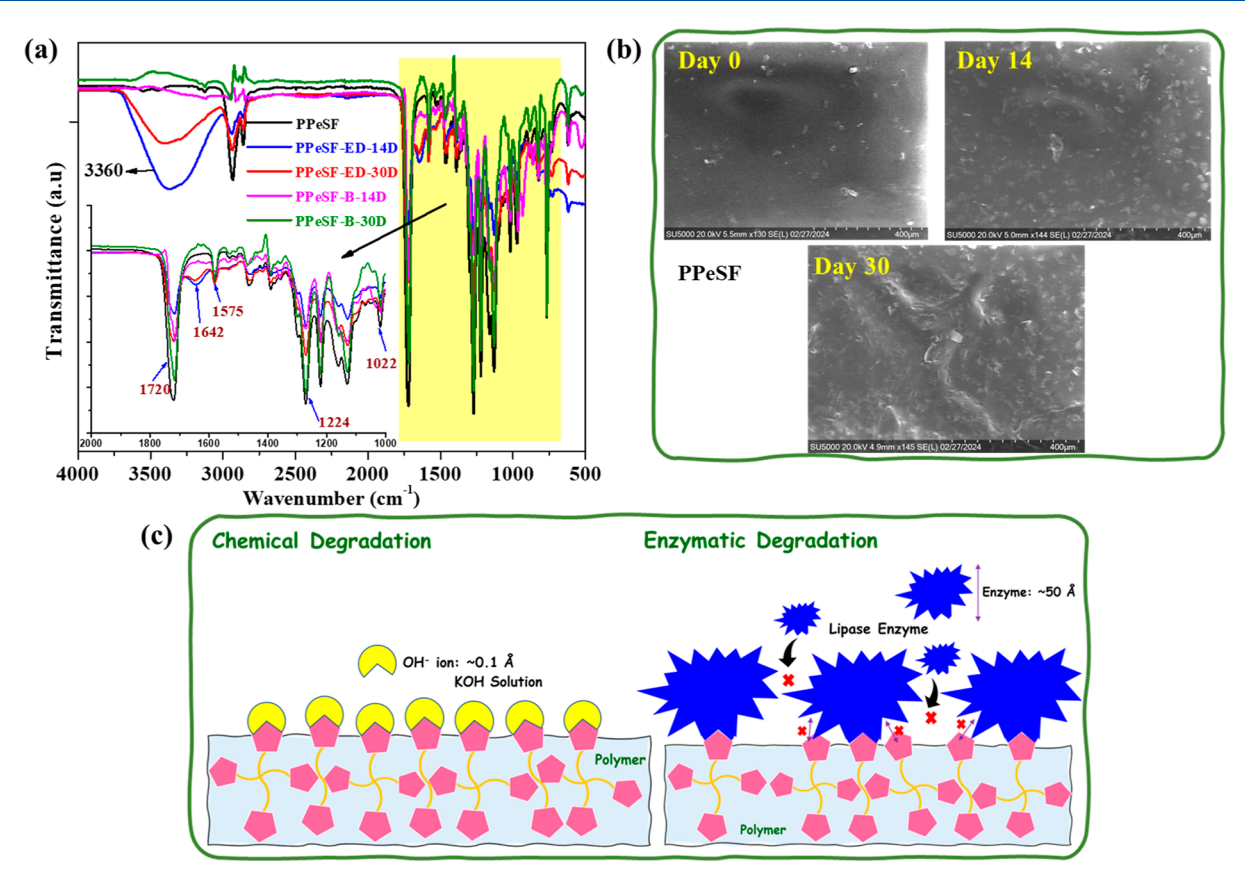


Figure 11. (a) FT-IR spectra and (b) SEM morphology of PPeSF during enzymatic degradation. (c) Schematics showing the chemical vs enzymatic degradation mechanism.

up the precise region of the substrate, thereby reducing the structural density of the polymer.

The biodegradability of the biobased polyester was also investigated in an aqueous chemical medium, where a 1 M NaOH solution at pH 13.0 was used. PPeSF copolyester was completely degraded within 5 days of dissolution time. The chemical degradation rate is observed to be faster than the enzymatic specificity. This phenomenon most likely has a strong correlation with the rate at which hydroxyl anions penetrate compared to enzyme specificity (Figure 11c). Compared to hydroxyl anions (effective ionic radius of 0.1 Å), 51 C. rugosa lipase enzyme is bulky in size (effective radius of ~ 50 Å) 52 and possesses a high propensity to form bimolecular aggregates, when the polymer target is properly docked onto aligned enzyme active sites. Consequently, C. rugosa lipase is a highly selective catalyst, because of its size and shape.

4. CONCLUSIONS

In summary, a series of fully biobased amorphous high molecular weight furan-based copolyesters, PBSF and PPeSF, utilizing biomass-derived monomers such as 1,4-butanediol or 1,5-pentanediol and dimethyl esters (dimethyl-2,5-furan dicarboxylate, DMS), were synthesized via a two-stage melt polycondensation process. All the synthesized copolyesters displayed an average molecular weight ($M_{\rm w}$) between 39,300 and 56,800 g/mol and intrinsic viscosity [η] from 0.67 to 1.07 dL/g. The fabricated polyesters exhibited different crystalline properties in terms of the DMF/glycol comonomer ratio. PBSF exhibited a semicrystalline nature with the appearance of a typical melting endotherm ($T_{\rm m}$) and low-intensity crystalline

peak, whereas PPeSF and PPeSF-70 (70 mol % of DMF) displayed an amorphous polymer nature. The odd-even number effect of PDO glycol subunits plays a vital role in determining the physical characteristics of the copolyesters. Despite being 100% biobased, PBSF or PPeSF demonstrated superior thermal stability (onset decomposition temperature higher than 370 °C) and good mechanical elasticity. PBSF compression-molded films were examined for tensile properties and exhibited a TS and elongation of 8.40 MPa and 617%, respectively, pretty much comparable to its terephthalate counterpart PBST (TS, elongation of 8.31 MPa and 497%). With an increase in the glycol chain length, PPeSF-70 also showed a remarkable elasticity of 584%, while the TS lowered to 6.82 MPa. Uniaxial stretching caused PBST to permanently distort, losing its mechanical qualities; yet, upon release, PBSF demonstrated an outstanding rebound (>70% elastic recovery), guaranteeing its durability over time. The rheological properties confirmed that the asymmetric, nonplanar furan ring structure and higher molecular weight of furan-derived polyesters underwent extensive chain entanglements compared to rigid and planar DMT-based terephthalate copolyesters, building up to higher elasticity. Moreover, PPeSF films exhibited biodegradability in both chemical and C. rugosa lipase enzyme medium, with an estimated 100% chemical degradation within 5 days and approximately 35% enzymatic degradation by 30 days.

According to these findings, furan-based copolyesters can outperform traditional PET or PBAT in terms of sustainability and performance, and their use in bottles and packaging appears to have no boundaries. Currently, FDCA is economically inferior to TPA in terms of cost, manufacturing,

and technology, making PBSF fabrication incomparable to PBST. However, the significance of FDCAs as a potential alternative to petroleum counterparts highlights the compound's potential to advance research and emerge as a key ingredient in biodegradable polymers.

AUTHOR INFORMATION

Corresponding Authors

Pranabesh Sahu — National Institute for Materials Advancement, Pittsburg State University, Pittsburg, Kansas 66762, United States; orcid.org/0000-0002-5010-3900; Email: pranabesh.cema@gmail.com

Ram K. Gupta — National Institute for Materials Advancement, Pittsburg State University, Pittsburg, Kansas 66762, United States; Department of Chemistry, Pittsburg State University, Pittsburg, Kansas 66762, United States; orcid.org/0000-0001-5355-3897;

Email: ramguptamsu@gmail.com

Authors

Lav Sharma – National Institute for Materials Advancement, Pittsburg State University, Pittsburg, Kansas 66762, United States; Department of Chemistry, Pittsburg State University, Pittsburg, Kansas 66762, United States

Tim Dawsey — National Institute for Materials Advancement, Pittsburg State University, Pittsburg, Kansas 66762, United States

Complete contact information is available at: https://pubs.acs.org/10.1021/acs.macromol.4c01066

Author Contributions

The manuscript was written through the contributions of all authors. All authors have approved the final version of the manuscript.

Notes

The authors declare no competing financial interest.

ACKNOWLEDGMENTS

The authors are grateful to the National Institute of Standards and Technology (NIST award number 70NANB20D146) and the U.S. Economic Development Administration (US-EDA award number 05-79-06038) for providing research infrastructure funding. The authors are grateful for the support from the National Science Foundation Award Number 2119754.

REFERENCES

- (1) Lau, W. W. Y.; Shiran, Y.; Bailey, R. M.; Cook, E.; Stuchtey, M. R.; Koskella, J.; Velis, C. A.; Godfrey, L.; Boucher, J.; Murphy, M. B.; et al. Evaluating scenarios toward zero plastic pollution. *Science* **2020**, 369, 1455–1461.
- (2) Plastics Europe. Plastics the Fact; Plastics Europe: Brussels, Belgium, 2019. www.plasticseurope.org (accessed March 2024).
- (3) Geyer, R.; Jambeck, J. R.; Law, K. L. Production, use, and fate of all plastics ever made. *Sci. Adv.* **2017**, 3 (7), No. e1700782.
- (4) Filiciotto, L.; Rothenberg, G. Biodegradable plastics: standards, policies, and impacts. *ChemSusChem* **2021**, *14*, 56–72.
- (5) Kim, M. S.; Chang, H.; Zheng, L.; Yan, Q.; Pfleger, B. F.; Klier, J.; Nelson, K.; Majumder, E. L.-W.; Huber, G. W. A Review of Biodegradable Plastics: Chemistry, Applications, Properties, and Future Research Needs. *Chem. Rev.* **2023**, *123*, 9915–9939.
- (6) Haider, T. P.; Völker, C.; Kramm, J.; Landfester, K.; Wurm, F. R. Plastics of the Future? The Impact of Biodegradable Polymers on the Environment and on Society. *Angew. Chem., Int. Ed.* **2019**, *58*, 50–62.

- (7) Rabnawaz, M.; Wyman, I.; Auras, R.; Cheng, S. A roadmap towards green packaging: the current status and future outlook for polyesters in the packaging industry. *Green Chem.* **2017**, *19*, 4737–4753.
- (8) Rameshkumar, S.; Shaiju, P.; O'Connor, K. E.; P, R. B. Bio-based and biodegradable polymers-State-of-the-art, challenges and emerging trends. *Curr. Opin. Green Sustainable Chem.* **2020**, *21*, 75–81.
- (9) Tullo, A. H. The biodegradable polymer PBAT is hitting the big time. Chem. Eng. News 2021, 99, 26–27.
- (10) Allied Market Research. Polybutylene Adipate Terephthalate Market Size, Share, Competitive Landscape and Trend Analysis Report, by Application: Global Opportunity Analysis and Industry Forecast, 2021–2030, 2021. https://www.researchandmarkets.com.
- (11) Mansoor, Z.; Tchuenbou-Magaia, F.; Kowalczuk, M.; Adamus, G.; Manning, G.; Parati, M.; Radecka, I.; Khan, H. Polymers Use as Mulch Films in Agriculture-A Review of History, Problems and Current Trends. *Polymers* **2022**, *14*, 5062.
- (12) Gandini, A.; Silvestre, A. J. D.; Neto, C. P.; Sousa, A. F.; Gomes, M. The furan counterpart of poly(ethylene terephthalate): An alternative material based on renewable resources. *J. Polym. Sci., Part A: Polym. Chem.* **2009**, 47, 295–298.
- (13) Sousa, A. F.; Vilela, C.; Fonseca, A. C.; Matos, M.; Freire, C. S. R.; Gruter, G. J. M.; Coelho, J. F. J.; Silvestre, A. J. D. Biobased polyesters and other polymers from 2,5-furan dicarboxylic acid: a tribute to furan excellency. *Polym. Chem.* **2015**, *6*, 5961–5983.
- (14) De Jong, E.; Dam, M. A.; Sipos, L.; Gruter, G.-J. M. Furandicarboxylic Acid (FDCA), A Versatile Building Block for a Very Interesting Class of Polyesters. In *Biobased Monomers, Polymers, and Materials*; Smith, P. B., Gross, R. A., Eds.; ACS Symposium Series, 2012: Vol. 1105...
- (15) Bozell, J. J.; Petersen, G. R. Technology development for the production of biobased products from biorefinery carbohydrates- the US Department of Energy's "Top 10" revisited. *Green Chem.* **2010**, *12*, 539–554
- (16) Khrouf, A.; Boufi, S.; Gharbi, R. E.; Belgacem, N. M.; Gandini, A. Polyesters bearing furan moieties. *Polym. Bull.* **1996**, *37*, 589–596.
- (17) Zhang, Z. H.; Deng, K. J. Recent advances in the catalytic synthesis of 2,5-furan dicarboxylic acid and its derivatives. *ACS Catal.* **2015**, *5*, 6529–6544.
- (18) Sajid, M.; Zhao, X. B.; Liu, D. H. Production of 2,5-furandicarboxylic acid (FDCA) from 5-hydroxymethylfurfural (HMF): recent progress focusing on the chemical-catalytic routes. *Green Chem.* **2018**, *20*, 5427–5453.
- (19) de Jong, E.; Visser, H. R. A.; Dias, A. S.; Harvey, C.; Gruter, G.-J. M. The Road to Bring FDCA and PEF to the Market. *Polymers* **2022**, *14* (5), 943.
- (20) Fei, X.; Wang, J.; Zhu, J.; Wang, X.; Liu, X. Biobased Poly(Ethylene 2,5-Furancoate): No Longer an Alternative, but an Irreplaceable Polyester in the Polymer Industry. *ACS Sustain. Chem. Eng.* **2020**, 8 (23), 8471–8485.
- (21) Burgess, S. K.; Leisen, J. E.; Kraftschik, B. E.; Mubarak, C. R.; Kriegel, R. M.; Koros, W. J. Chain Mobility, Thermal, and Mechanical Properties of Poly(Ethylene Furanoate) Compared to Poly(Ethylene Terephthalate). *Macromolecules* **2014**, *47*, 1383–1391.
- (22) Sun, L.; Wang, J.; Mahmud, S.; Jiang, Y.; Zhu, J.; Liu, X. New Insight into the Mechanism for the Excellent Gas Properties of Poly(Ethylene 2,5-Furandicarboxylate) (PEF): Role of Furan Ring's Polarity. *Eur. Polym. J.* **2019**, *118* (May), 642–650.
- (23) Papageorgiou, G. Z.; Papageorgiou, D. G.; Terzopoulou, Z.; Bikiaris, D. N. Production of bio-based 2,5-furan dicarboxylate polyesters: Recent progress and critical aspects in their synthesis and thermal properties. *Eur. Polym. J.* **2016**, 83, 202–229.
- (24) Guidotti, G.; Soccio, M.; García-Gutiérrez, M. C.; Ezquerra, T.; Siracusa, V.; Gutiérrez-Fernández, E.; Munari, A.; Lotti, N. Fully biobased superpolymers of 2,5-furandicarboxylic acid with different functional properties: from rigid to flexible, high performant packaging materials. ACS Sustainable Chem. Eng. 2020, 8, 9558–9568.
- (25) Zhu, J.; Cai, J.; Xie, W.; Chen, P. H.; Gazzano, M.; Scandola, M.; Gross, R. A. Poly(Butylene 2,5-Furan Dicarboxylate), a Biobased

- Alternative to PBT: Synthesis, Physical Properties, and Crystal Structure. *Macromolecules* **2013**, *46*, 796–804.
- (26) Lin, H.; Li, W.; Ou, Q.; Liu, J.; Wei, Z.; Wang, Z.; Shi, D.; Lei, W.; Zhang, L. Design and Characterization of High Gas Barrier and Fully Biobased Poly(1,5-pentylene succinate-co-itaconate-co-furanoate) Elastomers. ACS Sustainable Chem. Eng. 2024, 12 (14), 5640–5650.
- (27) Kim, H.; Kim, T.; Choi, S.; Jeon, H.; Oh, D. X.; Park, J.; Eom, Y.; Hwang, S. Y.; Koo, J. M. Remarkable elasticity and enzymatic degradation of bio-based poly (butylene adipate-co-furanoate): replacing terephthalate. *Green Chem.* **2020**, *22*, 7778–7787.
- (28) Lim, A. Y.; Park, S. B.; Choi, Y.; Oh, D. X.; Park, J.; Jeon, H.; Koo, J. M. Extending the high-performing boundaries of a fully biobased thermal shrinkage film targeted for food packaging applications. *Green Chem.* **2023**, *25*, 9711–9719.
- (29) Miah, M. R.; Dong, Y.; Wang, J.; Zhu, J. Recent Progress on Sustainable 2,5-Furandicarboxylate-Based Polyesters: Properties and Applications. ACS Sustainable Chem. Eng. 2024, 12 (8), 2927–2961.
- (30) Wang, Q.; Wang, J.; Dong, Y.; Zhang, X.; Hu, H.; Oyoung, L.; Hu, D.; Zhu, J. Synthesis of 2,5-furan dicarboxylic acid-based biodegradable copolyesters with excellent gas barrier properties composed of various aliphatic diols. *Eur. Polym. J.* 2022, *181*, 111677.
- (31) Poulopoulou, N.; Nikolaidis, G. N.; Ioannidis, R. O.; Efstathiadou, V. L.; Terzopoulou, Z.; Papageorgiou, D. G.; Kapnisti, M.; Papageorgiou, G. Z. Aromatic But Sustainable: Poly(butylene 2,5-furandicarboxylate) as a Crystallizing Thermoplastic in the Bioeconomy. *Ind. Eng. Chem. Res.* **2022**, *61* (36), 13461–13473.
- (32) Zubkiewicz, A.; Szymczyk, A.; Sablong, R. J.; Soccio, M.; Guidotti, G.; Siracusa, V.; Lotti, N. Bio-based aliphatic/aromatic poly (trimethylene furanoate/sebacate) random copolymers: Correlation between mechanical, gas barrier performances and compostability and copolymer composition. *Polym. Degrad. Stab.* **2022**, *195*, 109800.
- (33) Terzopoulou, Z.; Papadopoulos, L.; Zamboulis, A.; Papageorgiou, D. G.; Papageorgiou, G. Z.; Bikiaris, D. N. Tuning the properties of furandicarboxylic acid-based polyesters with copolymerization: A review. *Polymers* **2020**, *12* (6), 1209–1260.
- (34) Tsanaktsis, V.; Papageorgiou, G. Z.; Bikiaris, D. N. A facile method to synthesize high-molecular-weight biobased polyesters from 2,5-furandicarboxylic acid and long-chain diols. *J. Polym. Sci., Part A: Polym. Chem.* **2015**, *53*, 2617–2632.
- (35) Sousa, A. F.; Patrício, R.; Terzopoulou, Z.; Bikiaris, D. N.; Stern, T.; Wenger, J.; Loos, K.; Lotti, N.; Siracusa, V.; Szymczyk, A.; et al. Recommendations for replacing PET on packaging, fiber, and film materials with biobased counterparts. *Green Chem.* **2021**, 23 (22), 8795–8820
- (36) Kasmi, N.; Wahbi, M.; Papadopoulos, L.; Terzopoulou, Z.; Guigo, N.; Sbirrazzuoli, N.; Papageorgiou, G. Z.; Bikiaris, D. N. Synthesis and characterization of two new biobased poly (pentylene 2,5-furandicarboxylate-co-caprolactone) and poly (hexamethylene 2,5 furandicarboxylate-co-caprolactone) copolyesters with enhanced enzymatic hydrolysis properties. *Polym. Degrad. Stab.* **2019**, *160*, 242–263.
- (37) Chebbi, Y.; Kasmi, N.; Majdoub, M.; Cerruti, P.; Scarinzi, G.; Malinconico, M.; Dal Poggetto, G.; Papageorgiou, G. Z.; Bikiaris, D. N. Synthesis, characterization, and biodegradability of novel fully biobased poly (decamethylene-co-isosorbide 2,5-furandicarboxylate) copolyesters with enhanced mechanical properties. *ACS Sustain. Chem. Eng.* **2019**, *7* (5), 5501–5514.
- (38) Terzopoulou, Z.; Kasmi, N.; Tsanaktsis, V.; Doulakas, N.; Bikiaris, D. N.; Achilias, D. S.; Papageorgiou, G. Z. Synthesis and characterization of bio-based polyesters: poly(2-methyl-1,3-propy lene-2,5-furanoate), poly(isosorbide-2, 5-furanoate), poly (1,4-cyclo hexanedimethylene-2,5-furanoate). *Materials* **2017**, *10*, 801.
- (39) Wang, J.; Zhang, X.; Fei, X.; Gao, R.; Liu, F.; Fan, L.; Zhu, J.; Liu, X. Synthesis of High Thermal-Resistant Poly(ester-ether) Elastomers from Bio-Based 2,5-Furandicarboxylic Acid. ACS Sustainable Chem. Eng. 2022, 10 (41), 13595–13606.
- (40) Gao, R.; Wang, J.; Liu, F.; Dai, H.; Zhang, X.; Wang, X.; Li, Y.; Zhu, J. Synthesis of bio-based poly(ester-ether) elastomers from 2,5-

- furandicarboxylic acid (FDCA) with excellent thermo-mechanical properties. *Polym. Degrad. Stab.* **2023**, *210*, 110292.
- (41) Yang, T.; Liu, F.; Gao, R.; Zhang, X.; Li, J.; Wang, J.; Zhu, J. Fabrication of Thermoplastic Poly(ether-ester) Elastomers with High Melting Temperature and Elasticity from Bio-based 2,5-Furandicarboxylic Acid. ACS Sustainable Resour. Manage. 2024, 1, 1520–1533.
- (42) Huang, Y.; Su, W.; Lee, C. On the Weissenberg effect of turbulence. Theor. Appl. Mech. Lett. 2019, 9 (4), 236-245.
- (43) Lu, J.; Wu, L.; Li, B. High Molecular Weight Polyesters Derived from Biobased 1,5-Pentanediol and a Variety of Aliphatic Diacids: Synthesis, Characterization, and Thermo-Mechanical Properties. ACS Sustainable Chem. Eng. 2017, 5 (7), 6159–6166.
- (44) Sun, Y.; Wu, L.; Bu, Z.; Li, B.; Li, N.; Dai, J. Synthesis and Thermomechanical and Rheological Properties of Biodegradable Long-Chain Branched Poly (butylene succinate-co-butylene terephthalate) Copolyesters. *Ind. Eng. Chem. Res.* **2014**, *53* (25), 10380–10386.
- (45) Jang, S.; Yang, E. K.; Jin, S. I.; Cho, Y. D.; Choe, E. K.; Park, C. R. Characterization of Thermal Degradation of Polytrimethylene Terephthalate by MALDI-TOF Mass Spectrometry. *Bull. Korean Chem. Soc.* **2012**, *33*, 833–838.
- (46) Chen, S.; Chen, S.; Guang, S.; Zhang, X.; Chen, W. Film reaction kinetics for melt postpolycondensation of poly(ethylene terephthalate). *J. Appl. Polym. Sci.* **2020**, *137*, 48988.
- (47) Hu, X. R.; Shen, X. L.; Huang, M. F.; Liu, C. H.; Geng, Y. T.; Wang, R. G.; Xu, R. W.; Qiao, H.; Zhang, L. Q. Biodegradable unsaturated polyesters containing 2,3-butanediol for engineering applications: Synthesis, characterization and performances. *Polymer* 2016, 84, 343–354.
- (48) Wu, L. B.; Mincheva, R.; Xu, Y. T.; Raquez, J. M.; Dubois, P. High Molecular weight poly(butylene succinate-co-butylene furandicarboxylate) copolyesters: From catalyzed polycondensation reaction to thermomechanical properties. *Biomacromolecules* **2012**, *13*, 2973–2981.
- (49) Zheng, L.; Kim, M. S.; Xu, S.; Urgun-Demirtas, M.; Huber, G. W.; Klier, J. Biodegradable High-Molecular-Weight Poly(pentylene adipate-co-terephthalate): Synthesis, Thermo-Mechanical Properties, Microstructures, and Biodegradation. ACS Sustainable Chem. Eng. 2023, 11, 13885–13895.
- (50) Sahu, P.; Sharma, L.; Dawsey, T.; Gupta, R. K. Insight into the synthesis and thermomechanical properties of "short-long" type biobased aliphatic polyesters. *J. Appl. Polym. Sci.* **2023**, *141*, No. e54972.
- (51) Marcus, Y. Volumes of aqueous hydrogen and hydroxide ions at 0 to 200 °C. *J. Chem. Phys.* **2012**, *137*, 154501.
- (52) Domínguez de María, P.; Sánchez-Montero, J. M.; Sinisterra, J. V.; Alcántara, A. R. Understanding Candida rugosa lipases: An overview. *Biotechnol. Adv.* **2006**, *24*, 180–196.